Redshift of the He_α emission line of He-like ions under plasma environment

T. K. Fang,[1,*] C. S. Wu,[2] X. Gao,[2] and T. N. Chang[3]

[1]*Department of Physics, Fu Jen Catholic University, Taipei, Taiwan 242, ROC*

[2]*Beijing Computational Science Research Center, Beijing, 100084, China*

[3]*Department of Physics and Astronomy,*

University of Southern California, Los Angeles, CA 90089-0484, U.S.A.

Abstract

By carefully following the spatial and temporal criteria of the Debye-Hückel (DH) approximation, we present a detailed theoretical study on the redshifts of the spectroscopically isolated He_α lines corresponding to the $1s2p\ ^1P \rightarrow 1s^2\ ^1S$ emission from two-electron ions embedded in external dense plasma. We first focus our study on the ratio $R = \Delta\omega_\alpha/\omega_o$ between the redshift $\Delta\omega_\alpha$ due to the external plasma environment and the energy ω_o of the He_α line in the absence of the plasma. Interestingly, the result of our calculation shows that this ratio R turns out to vary as a nearly universal function of a reduced Debye length $\lambda_D(Z) = (Z-1)D$. Since the ratio R dictates the necessary energy resolution for a quantitative measurement of the redshifts and, at the same time, the Debye length D is linked directly to the plasma density and temperature, the dependence of R on D should help to facilitate the potential experimental efforts for a quantitative measurement of the redshifts for the He_α line of the two-electron ions. In addition, our study has led to a near constant redshift $\Delta\omega_\alpha$ at a given D for all He-like ions with Z between 5 and 18 based on our recent critical assessment of the applicability of the DH approximation to atomic transitions. These two general features, if confirmed by the observation, would offer a viable and easy alternative in the diagnostic efforts of the dense plasma.

PACS numbers: 32.30.Jc, 32.70.Jz, 52.25.Os

*Electronic address: 051420@mail.fju.edu.tw

I. INTRODUCTION

Experimentally, it has been observed that the low-lying Lyman α line of the H-like ions or the He_α lines of the two-electron ions, with their well-separated energies in the emission spectra, are red-shifted in laser-produced dense plasmas at an electronic temperature of a few hundred eV or less and at a density of the order of $10^{22}\ cm^{-3}$ or higher [1-4]. Such energy shifts, if well understood, could potentially lead to reliable diagnostic of laser produced high-density plasma [5]. Qualitatively, following the simple Debye-Hückel (DH) approximation [6-8], the redshift might be attributed to the upward shift of the atomic energy levels due to the screen-Coulomb potential in the presence of the external plasma environment. However, for the redshifts of the atomic spectral lines involving atomic energy levels close to the ionization threshold, one could not expect the DH approximation to work. This is partly due to the fact that the atomic electron responsible for such transition is located at a distance far away from the nucleus where the transition is expected to be strongly affected by the outside plasma and the DH model is in principle best suited for a classical electron-ion collisionless plasma under thermodynamic equilibrium, such as the gas discharged plasmas at relatively low density. Indeed, it was shown by Nantel *et al* [4] that near the series limit, the DH approximation breaks down. On the other hand, Fig. 1 of [4] also shows that the DH model appears to work qualitatively just like other more elaborated models for the spectral lines of H-like C^{5+} corresponding to transitions involving electron in the low n states.

It is well known that the application of the DH model depends on two key parameters. The first one is the radius A of the Debye sphere, which separates the affected outside plasma environment and the slightly modified close-in region where the atomic characteristic dominates. The second one is the Debye length D, which is related to the electron density N_e and temperature T of the outside plasma based on the classical Maxwell-Boltzmann statistics, or, more precisely in terms of the Bohr radius a_o by

$$D \ = \ 1.304 \times 10^9 \ (T/N_e)^{1/2} \ a_o, \tag{1}$$

where T and N_e are the plasma temperature (on Kelvin scale) and density (in cm^{-3}), respectively. Or, alternatively, for dense plasmas, it may be more convenient to express in terms of the electron energy kT in the units of eV and its density in the units of $1 \times 10^{22}\ cm^{-3}$

in terms of the expression of (see, also, e.g., Eq. (1-17) of [9])

$$D \;=\; 1.4048\;(kT/N_e)^{1/2}\;a_o. \tag{2}$$

A recent critical assessment of the DH approximation in terms of the spatial and temporal criteria for dense plasma [7] has shown that the DH approximation, with a careful choice of A, could generate the redshift of the Lyman α line of the H-like ion in plasma environment in agreement both with the experimentally observed value and the data from more elaborate simulations based on quantum mechanical approaches for ions with nucleus charge Z between 5 and 18. In addition, by applying the simple Z^2-scaling presented earlier, a straightforward extrapolation could generate the data for other ions from a single calculation for a reference ion [7]. We also note that the theoretical estimate of the atomic transitions leading to low-lying emission lines are essentially dictated by the inner most atomic orbits. This implies that the interaction is short-ranged in nature and is consistent with what we discussed earlier for DH approximation to apply. For the outside plasma to at least influence the inner most orbits, one should not assume too large a value of A to have little or no plasma influence on these orbits. At the same time, the value of A should not be too small either so that these inner orbits are exposed to the outside plasma field to the extent that it loses entirely the atomic characteristics. As a result, in simulating the redshifts of the low-lying emission lines within the framework of DH model, we have set the value of A comparable to the average size of the ion systems. Obviously, the DH model breaks down when $D \to A$. In fact, any reliable estimate of the plasma effect on atomic process based on DH model should be limited to Debye lengths that are somewhat longer than the radius A of the Debye sphere.

Whereas most of the diagnostic efforts on dense plasmas for low-lying emission lines are focused on the change of the line profile due to complicated collisional processes, the main objective of this paper is to offer an alternative by extending our earlier work on the plasmas of the H-like ions [7] with a similar analysis for the redshifts of the He_α line of the two-electron ions. We will examine in detail the ratio R of the redshift $\Delta\omega_\alpha$ to the energy of the He_α line ω_o in the absence of the external plasma, i.e., $R = \Delta\omega_\alpha/\omega_o$, as a function of the Debye length D. The ratio R is linked intimately to the experimental energy resolution which determines the prospect of quantitative observation of the redshift. Just like what we concluded for the H-like ions, we will present the dependence of R on a modified reduced Debye length $\lambda_D(Z) = (Z-1)D$, similar to the reduced Debye length defined by Eq.(8)

of [7], and the possibility to extrapolate the numerical data from a reference ion to other ions embedded in the dense plasmas. In Section II, we outline the theoretical procedures leading to our numerical calculation. In Section III, our results for ions with relatively low Z between 5 and 18 are presented. We will also show the effect due to the relativistic interactions for heavier He-ions (e.g., with Z greater than 50), when the DH model is once again applicable based on the spatial and temporal criteria. Finally, in Section IV, we will discuss the possible experimental implication of the present work.

II. THEORETICAL PROCEDURE BASED ON THE DEBYE-HÜCKEL APPROXIMATION

The numerical results presented in Sec. III are calculated with the B-spline-based configuration (BSCI) method which has been applied successfully to a large number of atomic structure properties [10, 11]. Details of the theoretical approach, the computational procedure, and its applications have already been presented in details elsewhere [10]. The energies of the atomic states are calculated typically with a basis set representing over 10,000 two-electron configurations with contributions from both positive and negative energy atomic orbitals. Following the original Debye-Hückel approximation, the two-electron orbital functions are constructed with individual one-electron atomic orbitals generated from an effective one-electron Hamiltonian $h_o(r, D)$, i.e.,

$$h_o(r; D) = \frac{p^2}{2m} + V_d(r; D), \tag{3}$$

where p is the momentum of the electron and $V_d(r; D)$ is a potential subject to a charge-neutral electron-ion plasma at a distance r from the nuclear charge Z given by [12, 13]

$$V_d(r; D) = \begin{cases} V_i(r) = -Ze^2(\frac{1}{r} - \frac{1}{D+A}), & r \leq A \\ \\ V_o(r) = -Ze^2(\frac{De^{A/D}}{D+A})\frac{e^{-r/D}}{r}, & r \geq A. \end{cases} \tag{4}$$

For simplicity, nearly all other recent applications [14-20] of the DH approximation to atomic processes were carried out in the limit when $A \to 0$, instead of V_d, i.e., with a screened Coulomb potential V_s

$$V_s(r; D) = -\frac{Ze^2}{r}e^{-r/D}. \tag{5}$$

The N-electron Hamiltonian for an atom in plasma environment in the present calculation is expressed in terms of $h_o(r;D)$ as [8]

$$H(r_i, r_j, \cdots; D) = \sum_{i=\ 1,N} h_o(r_i; D) + \sum_{i>j}^{N} \frac{e^2}{r_{ij}}, \tag{6}$$

where $r_{ij} =\mid \vec{r_i} - \vec{r_j} \mid$ represents the separation between the atomic electrons i and j. By diagonalizing the Hamiltonian matrix with basis set of multiconfiguration two-electron orbitals discussed earlier and following the numerical procedure detailed elsewhere [8, 10], the energy of the He_α line under the external plasma environment in terms of the Debye length D is given by the difference of the energies between the $1s^2\ ^1S$ ground state and the $1s2p\ ^1P$ first excited state, i.e.,

$$\omega_\alpha(D) = \epsilon_{1s2p\ ^1P}(D) - \epsilon_{1s^2\ ^1S}(D). \tag{7}$$

The energy of the He_α line in the absence of the external plasma is given by $\omega_o = \omega_\alpha(D = \infty)$ and the red-shift $\Delta\omega_\alpha$ is thus given by

$$\Delta\omega_\alpha(D) = \omega_o - \omega_\alpha(D). \tag{8}$$

For relativistic calculations, the N-electron Hamiltonian for an atom in plasma environment in the present calculation is expressed as

$$H^{\ DC} = \sum_{i=\ 1,N} [\ c\ \vec{\alpha} \cdot \vec{p_i} + (\beta - 1)mc^2 + V_d(r_i; D)\ ] + \sum_{i>j}^{N} \frac{e^2}{r_{ij}}, \tag{9}$$

where $\alpha_k = \begin{pmatrix} 0 & \sigma_k \\ \sigma_k & 0 \end{pmatrix}$ with $k = (1, 2, 3)$, σ_k is the Pauli 2×2 matrix, and $\beta = \begin{pmatrix} I & 0 \\ 0 & -I \end{pmatrix}$ with I the 2×2 unit matrix. The calculations were carried out using a revised multi-configuration Dirac-Fock (MCDF) approach which takes the electron correlations into account. The quasi-complete basis scheme [21, 22] is adopted to optimize the atomic orbitals (AOs) using the GRASP_JT version based on the earlier GRASP2K codes [23] with the highest principal number of the AOs up to $n_{max} = 5$. The only difference from the earlier calculation is the use of $V_d(r;D)$ instead of the one-electron potential $-Ze^2/r$ in Eq.(9) under the DH approximation. All other computational procedures leading to ω_o and $\Delta\omega_\alpha(D)$ are the same as the non-relativistic calculations outlined earlier.

III. RESULTS AND DISCUSSIONS

We started the present study by choosing first the value of A in terms of the average radius of one of the electrons in the ground state of He-like ions, denoted as $< r >_{1s}$ in terms of a parameter η by

$$A = \eta < r >_{1s} . \tag{10}$$

Similar to our recently reported estimate of the redshift of the Lyman-α emission lines for the H-like ions in dense plasmas [7], the calculated ratio $R = \Delta\omega_\alpha/\omega_o$ presented in Fig. 1 as functions of the reduced Debye length $\lambda_D(Z) = (Z-1)D$ also vary substantially for different radii of Debye sphere, e.g., in the present calculation, from $A = 0$ to $A = 2 < r >_{1s}$ for He-like C, Ne, Mg, and Ar ions, respectively. The nearly universal dependence of R on λ_D shown in Fig. 1 is in fact expected since both ω_o and $\Delta\omega_\alpha$ scale as Z_{eff}^2 similar to the Z^2 scaling for H-like ions discussed in [7]. We have chosen the values of λ_D leading to R with values ranging from approximately 0.1% to about 6%, close to an energy resolution that may accommodate the experimental observation. Table I presents the calculated R in % for He-like Mg ion in dense plasma as functions of λ_D for the three radii $A = 0$, $A =< r >_{1s}$ and $A = 2 < r >_{1s}$, respectively. The nearly universal dependence of R on λ_D shown in Fig. 1 offers the possibility of simple extrapolation of R from the reference data set for the He-like Mg ion to other ions. Figure 2 presents an excellent agreement between the extrapolated data from Table I and the directly calculated data for Ar^{16+} and Ne^{8+} ions at three radii $A = 0\,(\eta = 0)$, $A =< r >_{1s}\,(\eta = 1)$, and $A = 2 < r >_{1s}\,(\eta = 2)$, respectively.

Another interesting general feature for the redshifts based on the DH approximation is a near constant $\Delta\omega_\alpha$ (within a few percents) for the He-like ions subject to outside dense plasma at a specific Debye length D shown in Table II. Qualitatively, $\Delta\omega_\alpha$ is given approximately by the difference in energy corrections for a quasi-hydrogenic H-like ions between the $1s$ and $2p$ levels due to the difference in pure Coulomb potential and the screening Coulomb potential, i.e., $\Delta V_D = (Ze^2/r)(1 - e^{-r/D})$. The redshift $\Delta\omega_\alpha$ at a given D and Z could be estimated qualitatively by the difference of the expectation values of $< 1s \mid \Delta V_D \mid 1s >$ and $< 2p \mid \Delta V_D \mid 2p >$. It is straightforward to show analytically that the estimated redshift $\Delta\omega_\alpha$ is given approximately by

$$\Delta\omega_\alpha \approx \frac{7}{4}\frac{1}{D^2} - \frac{9}{2Z}\frac{1}{D^3} \tag{11}$$

with a leading term independent of Z and varies as $1/D^2$. The numerical values listed in Table II indeed decrease approximately as $1/D^2$ as D increases. Since Debye length D is the key parameter that links the temperature and electron density of the dense plasma, together with its link to the the near-constant redshift, the plots presented in Fig. 3 could facilitate an easy road map to the potential redshifts measurement. In essence, each curve corresponding to a specific D represents the near constant redshift for all He-like ions that fits the basic criteria of DH approximation. Assuming that the experimental energy resolution is sufficient to resolve the redshift, each of the curve offers the possible temperature and density combination for measurement. Or, if the density and temperature are already well characterized for the dense plasma, one could determine what energy resolution is required to observe the redshift.

Although a few dense plasma experiment have been performed at a plasma density as high as 1-10 g/cc (e.g., see [1] for Al ions) or an electron density of the order of 10^{24} cm^{-3}, most of the existing dense plasma measurements are carried out at a density N_e of the order of 10^{22} cm^{-3} or less. As a result, based on the data presented in Figs. 1 and 3, to realistically measure the redshifts, we will examine $R = \Delta\omega_\alpha/\omega_o$ at D greater than 6 a_o, or with λ_D beyond those presented in Fig. 1. Figure 4 presents two such plots of R at $kT =$ 150 eV with N_e up to 10^{23} cm^{-3} for Mg ion and at $kT = 600$ eV with N_e up to 10^{24} cm^{-3} for Al ion, respectively. Clearly, with kT and N_e closer to the readily available experimental conditions, the energy resolution, according to the value of R, needs to be improved to one over thousand or better if the redshifts are to be measured quantitatively.

We now turn our attention to the effect on redshifts due to the relativistic interactions. In Fig. 5, the expectation that the redshift of the He_α emission line due to the external plasma of low Z ion is not affected by the relativistic interactions is confirmed by the nearly identical values of R between the ones calculated for the He-like O ion, with relativistic interactions included, and the non-relativistic universal curve shown earlier. For the intermediate Z, the DH approximation does not work well due to the spatial and temporal criteria discussed earlier [7]. As Z increases further, the DH approximation should work once again. The effect of the relativistic interaction could clearly be seen in Fig. 5 from the difference in R values between the relativistic calculation and the non-relativistic ones extrapolated from the universal curve shown in Fig. 1 for the He-like Yb and Au ions.

IV. CONCLUSION

By focusing on the ratio $R = \Delta\omega_\alpha/\omega_o$ of the redshift $\Delta\omega_\alpha$ to the energy ω_o of the He_α line in the absence of the external plasma, we are able to show that the ratio R varies as a nearly universal function of the reduced Debye length λ_D shown in Fig. 1 for all He-like ions embedded in the external plasmas that meet the spatial and temporal criteria of the Debye-Hückel approximation. This universal feature based on the simple DH approximation in terms of the Debye length D offers the critical links between the redshifts of He_α emission lines to the key experimental parameters, including the density and temperature of the external dense plasma and the required energy resolution of the spectrometer for experimental observation. Our study has also led to a second general feature based on the DH approximation with a near-constant value of the redshift for all He-like ions that varies approximately as $1/D^2$ as listed in Table II. The simulated numerical data for the redshifts presented in Sec. III, nevertheless, vary approximately by a factor close to three as the radius of the Debye sphere changes from $A = 0$ to $A = 2 < r >_{1s}$ shown in Figs. 1, 2, and 4 as well as in Tables I and II.

Some of the experimental set-ups have already generated the plasmas with densities up to 10^{23} cm^{-3} or higher at a few hundreds eV, which meet the required plasma environment that the redshifts are sufficiently large to be measured quantitatively. As for the energy resolution, it has also been improved substantially in recent years. For example, up to $E/\Delta E$ of 3000 for monochromator is available for energies from 500 to 1000 eV and a bit lower for energy up to 2000 eV with the SXR (soft x-ray material science) instrument at Linac Coherent Light Source (LCLS) free electron laser (FEL) [24]. One of the main objectives of this paper is to generate the necessary impetus for new experiments with proper plasma conditions and adequate energy resolution that are sufficient for quantitatively measured redshifts of the low-lying atomic spectral lines from He-like ions subject to outside plasmas. Measured data from such experiments, together with the estimated data presented in this paper, would lead to a better assessment of the radius of Debye sphere for a more reliable quantitative estimation of the redshifts of low-lying atomic emission lines and, in turn, offer a viable alternative in the diagnostic efforts of dense plasmas in addition to the change of the spectral profiles of the emission lines.

Acknowledgments

This work was supported by the MOST in Taiwan under Grant No. MOST 105-2112-M-030-004, the National Natural Science Foundation of China under Grant Nos. U1530401 and 11774023, the Special Program for Applied Research on Super Computation of the NSFC-Guangdong Joint Fund, the National High-Tech ICF Committee in China. We also acknowledge the computational support from the Beijing Computational Science Research Center (CSRC). In addition, TNC is thankful for the partial support from NCTS in Taiwan.

---

[1] D. J. Hoarty *et al*, Phys. Rev. Lett. **110**, 265003 (2013).

[2] A. Saemann *et al*, Phys. Rev. Lett. **82**, 4843 (1999); R. C. Elton, J. Ghosh, H. R. Griem, and E. J. Iglesias, Phys. Rev. E **69**, 067403 (2004).

[3] Y. Leng, J. Goldhar, H. R. Griem, and R. W. Lee, Phys. Rev. E **52**, 4328 (1995).

[4] M. Nantel, G. Ma, S. Gu, C. Y. Côté, J. Itatani, and D. Umstadter, Phys. Rev. Lett. **80**, 4442 (1998).

[5] S. Skupsky, Phys. Rev. A **21**, 1316 (1980).

[6] P. Debye and E. Hückel, Phyzik Z. **24**, 185 (1923).

[7] T. N. Chang, T. K. Fang, and X. Gao, Phys. Rev. A **91**, 063422 (2015).

[8] T. N. Chang and T. K. Fang, Phys. Rev. A **88**, 023406 (2013).

[9] F. F. Chen, in *Introduction to Plasma Physics and Controlled Fusion, Vol. 1, Plasma Physics*, 2nd ed. (Springer Science, Berlin/Heidelberg/NY, 2006).

[10] T. N. Chang, in *Many-body Theory of Atomic Structure and Photoionization*, edited by T. N. Chang (World Scientific, Singapore, 1993), p. 213.

[11] T. N. Chang and T. K. Fang, Radiat. Phys. Chem. **70**, 173 (2004); T. N. Chang and T. K. Fang, Phys. Rev. A **52**, 2638 (1995); T. N. Chang and X. Tang, Phys. Rev. A **44**, 232 (1991); T. N. Chang, Phys. Rev. A **39**, 4946 (1989).

[12] C. A. Rouse, Phys. Rev. **163**, 62 (1967).

[13] H. Margenau and M. Lewis, Rev. Mod. Phys. **31**, 569 (1959).

[14] S. Bhattacharyya, A. N. Sil, S. Fritzsche, and P. K. Mukherjee, Eur. Phys. J. D **46**, 1 (2008).

[15] A. N. Sil and P. K. Mukherjee, Int. J. Quantum. Chem. **102**, 1061 (2005); P. K. Mukherjee,

J. Karwowski, and G. H. F. Diercksen, Chem. Phys. Lett. **363**, 323 (2002).

[16] H. Okutsu, T. Sako, K. Yamanouchi, and G. H. F. Diercksen, J. Phys. B **38**, 917 (2005).

[17] S. B. Zhang, J. G. Wang, and R. K. Janev, Phys. Rev. A **81**, 032707 (2010); Phys. Rev. Lett. **104**, 023203 (2010); Y. Y. Qi, Y. Wu, J. G. Wang, and Y. Z. Qu, Phys. Plasmas **16**, 023502 (2009).

[18] C. Y. Lin and Y. K. Ho, Comp. Phys. Comm. **182**, 125 (2011); C. Y. Lin and Y. K. Ho, Eur. Phys. J. D **57**, 21 (2010); S. Sahoo and Y. K. Ho, J. Quant. Spectrosc. Radiat. Trans. **111**, 52 (2010); S. Kar and Y. K. Ho, J. Quant. Spectrosc. Radiat. Trans. **109**, 445 (2008); S. Kar and Y. K. Ho, Phys. Plasmas **15**, 013301 (2008); S. Kar and Y. K. Ho, Int. J. Quantum Chem. **106**, 814 (2006); A. Ghoshal and Y. K. Ho, J. Phys. B **42**, 075002 (2009); A. Ghoshal and Y. K. Ho, J. Phys. B **42**, 175006 (2009).

[19] Z. Wang and P. Winkler, Phys. Rev. A **52**, 216 (1995); S. T. Dai, A. Solovyova, and P. Winkler, Phys. Rev. E **64**, 016408 (2001).

[20] X. Lopez, C. Sarasola, and J. M. Ugalde, J. Phys. Chem. A **101**, 1804 (1997).

[21] X. Y. Han, X. Gao, D. L. Zeng, J. Yan, and J. M. Li, Phys. Rev. A **85**, 062506 (2012); X. Y. Han, X. Gao, D. L. Zeng, R. Jin, J. Yan, and J. M. Li, Phys. Rev. A 89, 042514 (2014); X. Gao, X. Y. Han and J. M. Li, J. Phys. B **49**, 214005 (2016).

[22] X. Gao, X. Y. Han, D. L. Zeng, R. Jin, and J. M. Li, Phys. Lett. A **378**, 1514 (2014).

[23] P. Jonsson, X. He, C. Froses Fischer, and I. P. Grant, 2007 Comput. Phys. Commun. **177**, 597 (2007).

[24] P. Heimann *et al*, Rev. Scient. Instru. **82**, 093104 (2011).

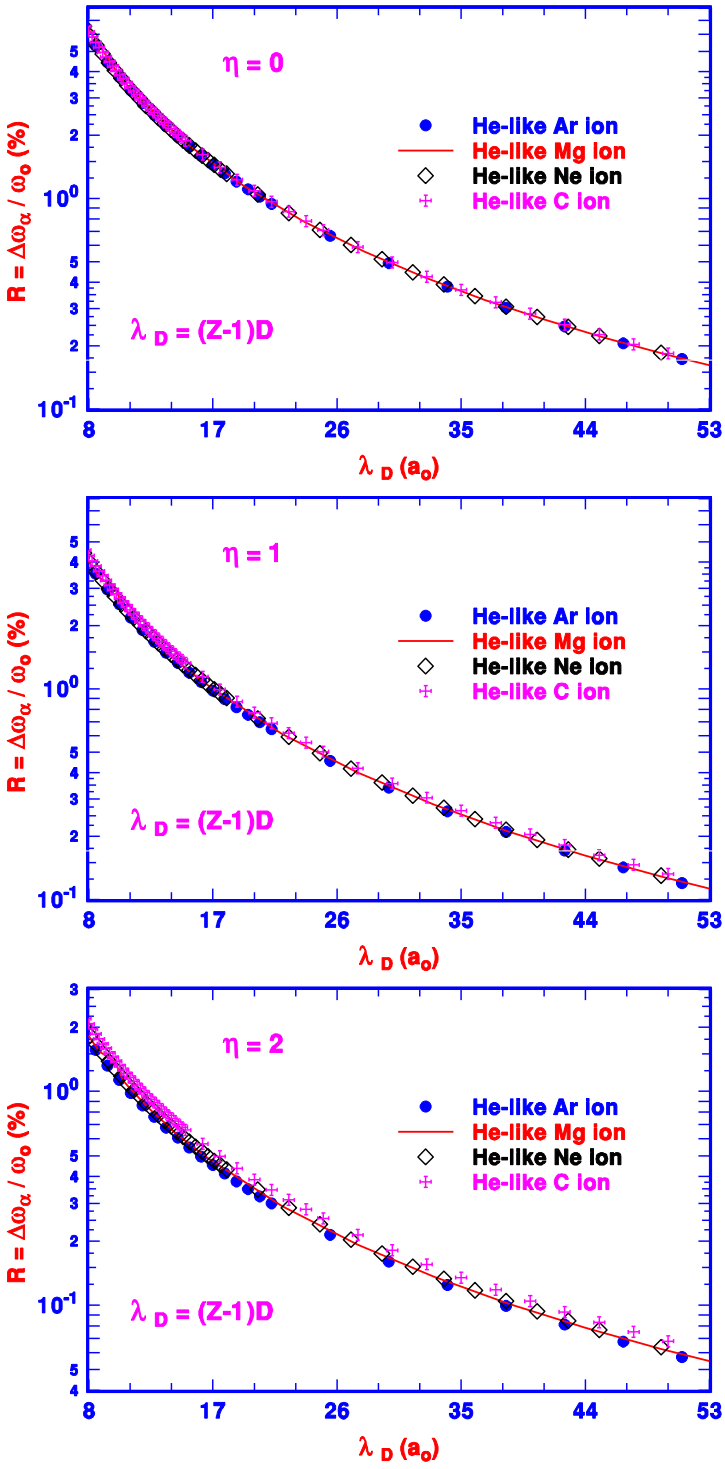

FIG. 1: The ratio R in percentage as functions of reduced Debye length $\lambda_D(Z) = (Z-1)D$ calculated with three radii of Debye sphere.

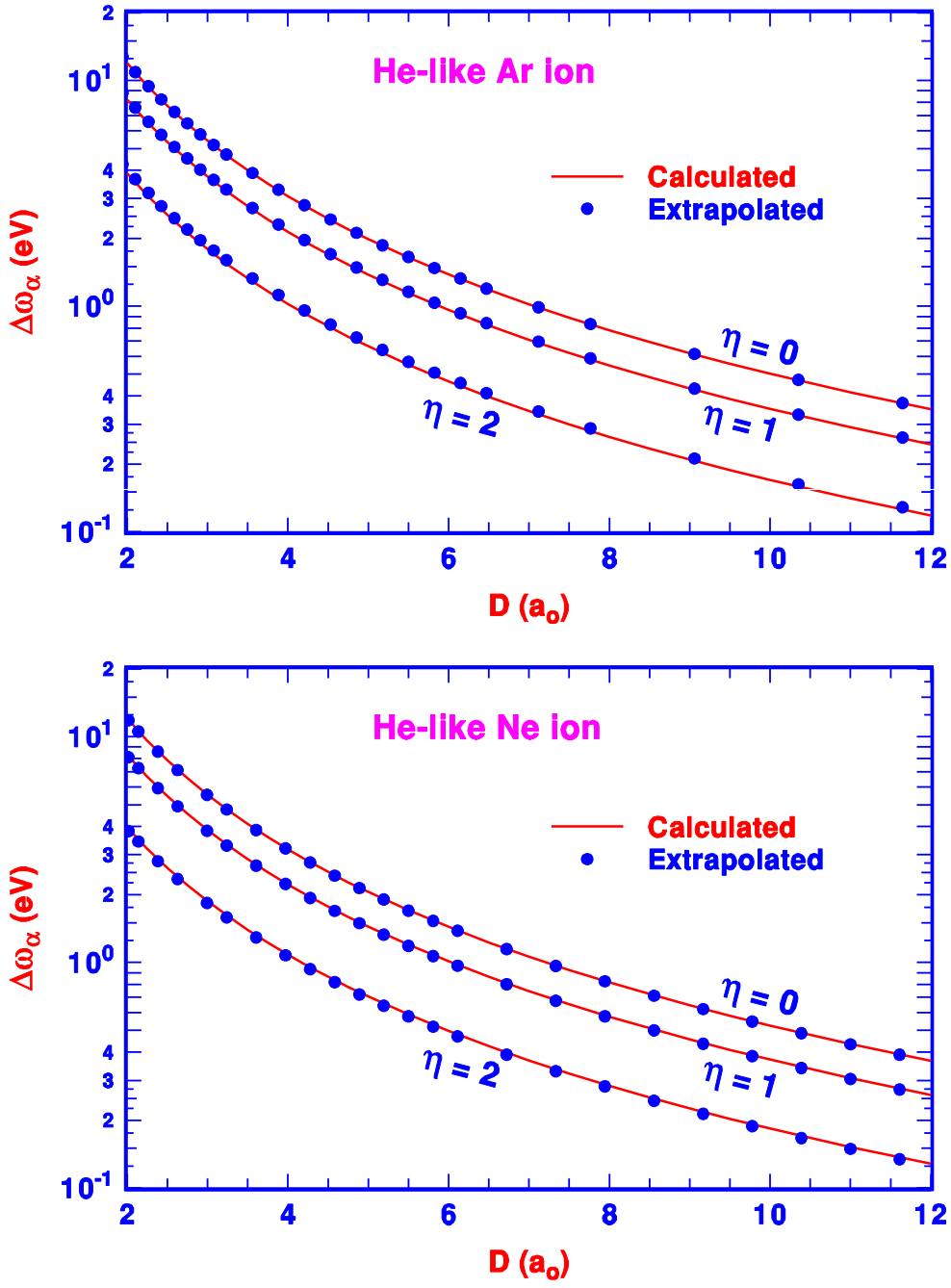

FIG. 2: The redshifts $\Delta\omega_\alpha$ in eV as functions of Debye length D calculated with three radii of Debye sphere for He-like Ar and Ne ions embedded in dense plasma. The calculated values of $\Delta\omega_\alpha$ are in excellent agreement with the extrapolated ones from the referenced data for He-like Mg ions.

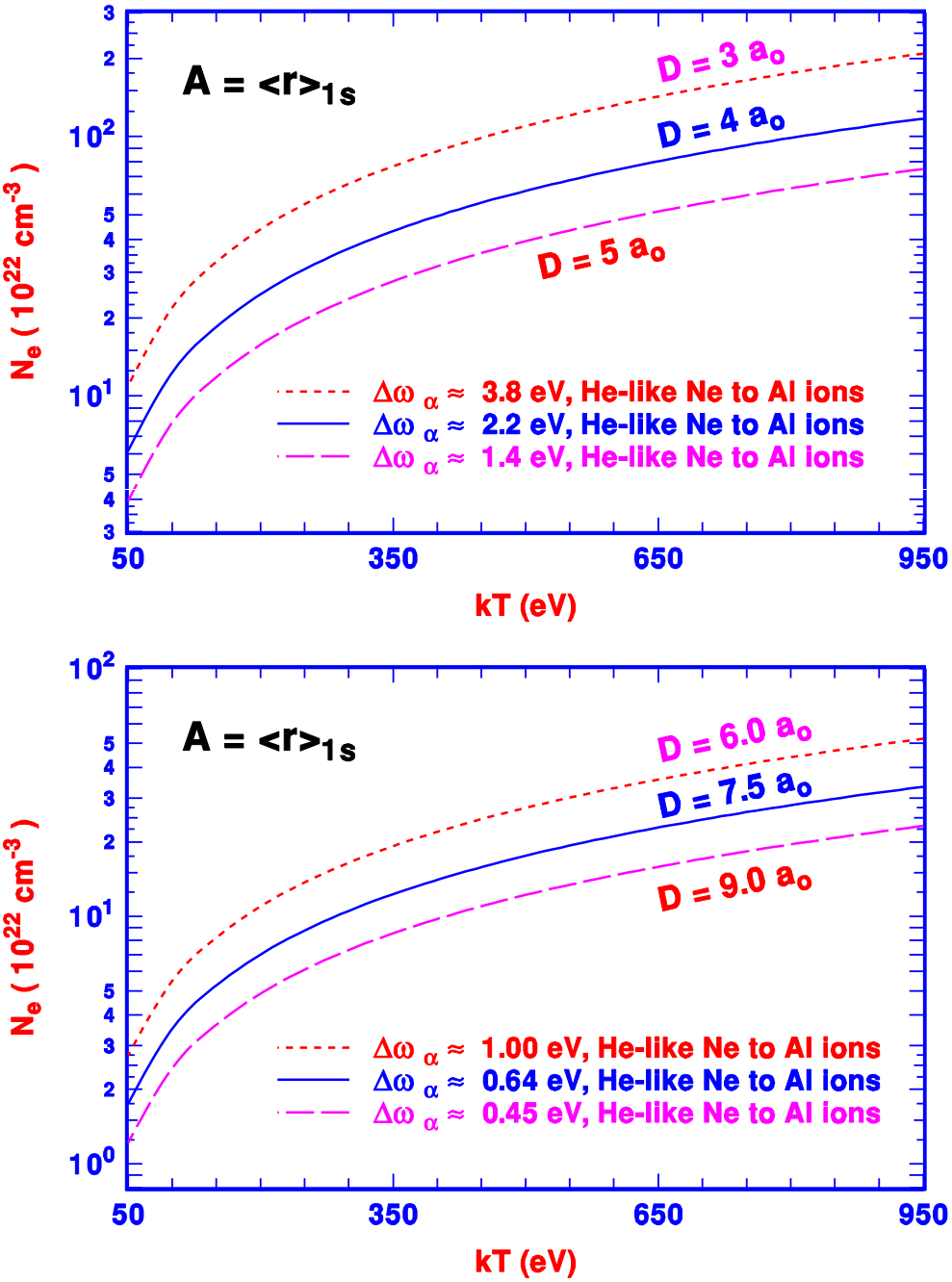

FIG. 3: Density N_e vs. temperature kT at a given Debye length D. For a given Debye length D, the redshifts $\Delta\omega_\alpha$ of the He_α lines are close to a constant value for all He-like ions.

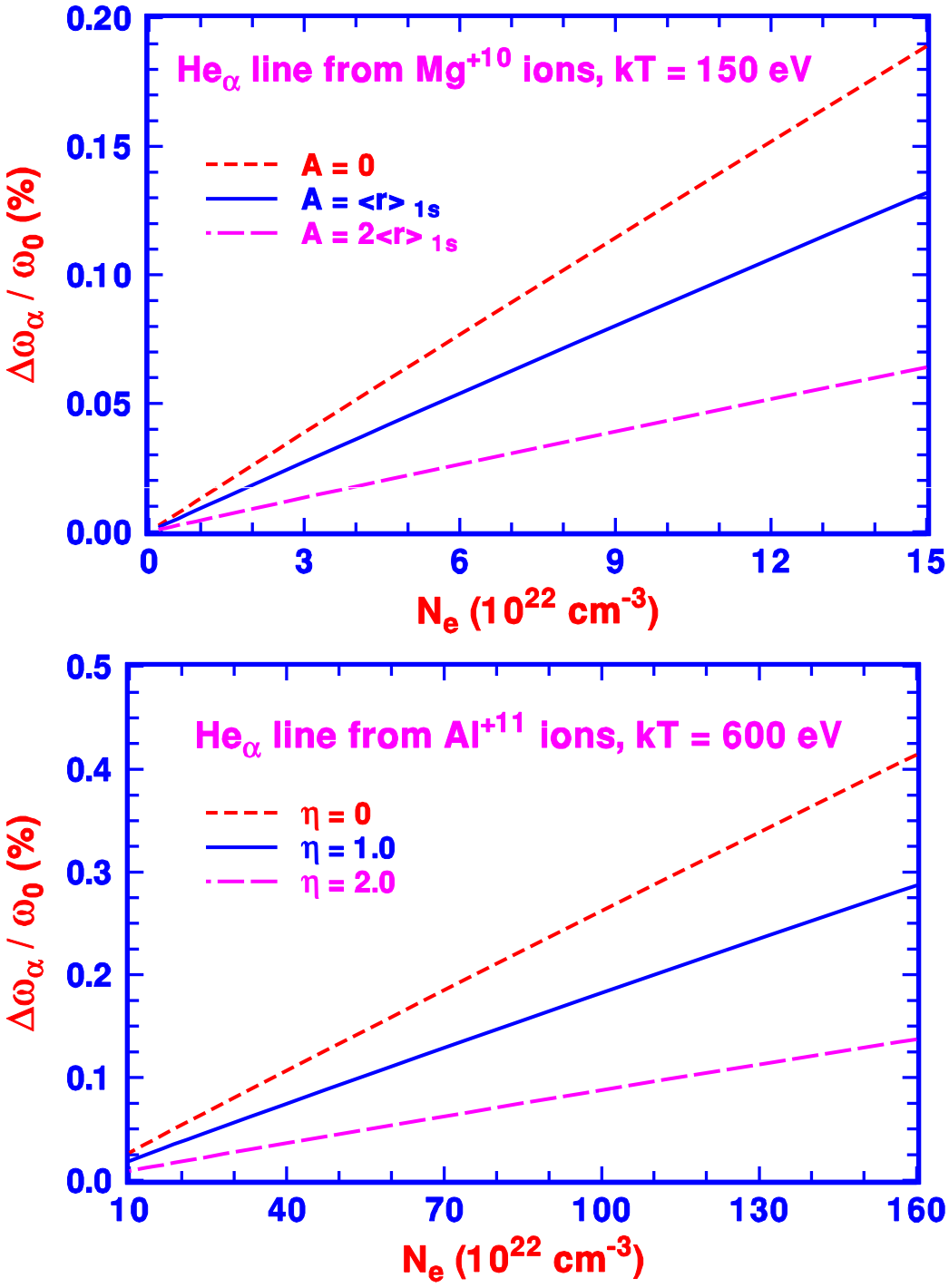

FIG. 4: $\Delta\omega_\alpha/\omega_o$ at $kT = 150$ eV with N_e up to 1.5×10^{23} cm^{-3} for Mg ions and at $kT = 600$ eV with N_e up to 1.6×10^{24} cm^{-3} for Al ions.

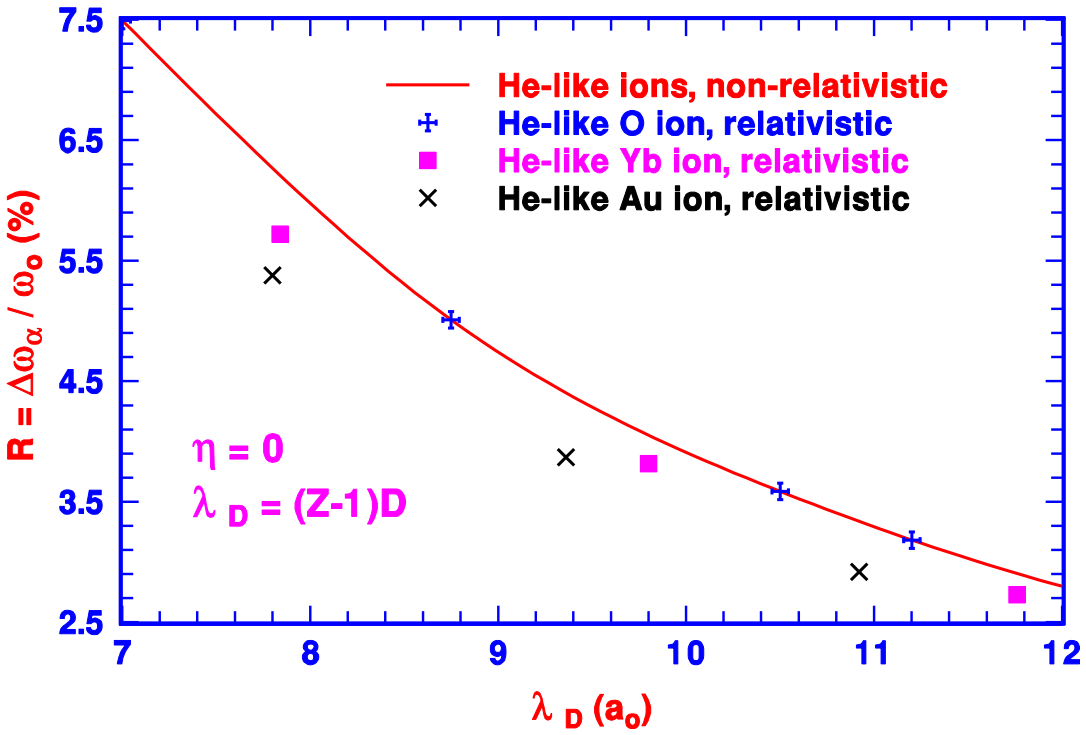

FIG. 5: Comparison between the relativistic calculation and the non-relativistic ones represented by the universal curve shown in Fig. 1.

TABLE I: The percentage of redshifts of He_α line of He-like Mg ion in dense plasma as functions of the *reduced* Debye Length $\lambda_D = (Z-1)D$ for $A = 0, A =< r >_{1s}$, and $A = 2 < r >_{1s}$, respectively.

D	λ_D (a_o)	R $[a(n) = a \times 10^n$ %]		
		$A = 0$	$A =< r >_{1s}$	$A = 2 < r >_{1s}$
5.50	60.50	1.24 (-1)	8.70 (-2)	4.24 (-2)
5.00	55.00	1.50 (-1)	1.05 (-1)	5.10 (-2)
4.50	49.50	1.84 (-1)	1.29 (-1)	6.25 (-2)
4.00	44.00	2.32 (-1)	1.62 (-1)	7.84 (-2)
3.50	38.50	3.01 (-1)	2.10 (-1)	1.01 (-1)
3.00	33.00	4.06 (-1)	2.82 (-1)	1.36 (-1)
2.50	27.50	5.78 (-1)	4.00 (-1)	1.92 (-1)
2.00	22.00	8.87 (-1)	6.12 (-1)	2.91 (-1)
1.50	16.50	1.54 (0)	1.05 (0)	4.94 (-1)
1.45	15.95	1.64 (0)	1.12 (0)	5.26 (-1)
1.40	15.40	1.75 (0)	1.20 (0)	5.60 (-1)
1.35	14.85	1.88 (0)	1.28 (0)	5.99 (-1)
1.30	14.30	2.01 (0)	1.37 (0)	6.41 (-1)
1.25	13.75	2.17 (0)	1.48 (0)	6.88 (-1)
1.20	13.20	2.34 (0)	1.59 (0)	7.41 (-1)
1.15	12.65	2.54 (0)	1.73 (0)	8.00 (-1)
1.10	12.10	2.76 (0)	1.87 (0)	8.67 (-1)
1.05	11.55	3.01 (0)	2.04 (0)	9.42 (-1)
1.00	11.00	3.30 (0)	2.23 (0)	1.03 (0)
0.95	10.45	3.64 (0)	2.46 (0)	1.13 (0)
0.90	9.90	4.02 (0)	3.01 (0)	1.37 (0)
0.80	8.80	5.01 (0)	3.37 (0)	1.53 (0)
0.75	8.25	5.66 (0)	3.79 (0)	1.72 (0)
0.70	7.70	6.43 (0)	4.30 (0)	1.94 (0)
0.65	7.15	7.39 (0)	4.93 (0)	2.21 (0)
0.60	6.60	8.59 (0)	5.72 (0)	2.55 (0)
0.55	6.05	1.01 (1)	6.72 (0)	2.98 (0)

TABLE II: The redshifts $\Delta\omega_\alpha$ in eV of the He_α line for a number of He-like ions embedded in dense plasma as functions of the Debye Length D.

$D(a_o)$	Ne^{8+}	Mg^{10+}	Al^{11+}
	$\omega_\alpha(D=\infty)=921.2\ eV$	$\omega_\alpha(D=\infty)=1350.2\ eV$	$\omega_\alpha(D=\infty)=1595.4\ eV$
		$A=0\ (\eta=0)$	
9	0.646	0.635	0.631
7.5	0.925	0.911	0.905
6	1.435	1.414	1.406
5	2.050	2.023	2.013
4	3.168	3.131	3.117
3	5.531	5.481	5.463
		$A=<r>_{1s}\ \ (\eta=1)$	
9	0.456	0.446	0.443
7.5	0.652	0.639	0.634
6	1.009	0.991	0.984
5	1.440	1.415	1.406
4	2.218	2.185	2.172
3	3.854	3.809	3.792
		$A=2<r>_{1s}\ \ (\eta=2)$	
9	0.225	0.218	0.216
7.5	0.322	0.313	0.309
6	0.496	0.483	0.478
5	0.706	0.688	0.682
4	1.082	1.058	1.050
3	1.866	1.833	1.821